Rend. Istit. Mat. Univ. Trieste
Volume 52 (2020), 1–21 (electronic preview)
DOI: 10.13137/2464-8728/30916

Numerical global bifurcation diagrams for a superlinear indefinite problem with a parameter appearing in the domain

Andrea Tellini

To Julián López-Gómez, on the occasion of his 60^{th} birthday, with deep gratitude and my best wishes for many more years of mathematical creativity, in the art of moving parameters

Abstract. *We consider a superlinear indefinite problem with homogeneous Neumann boundary conditions and a parameter appearing in the domain of the differential equation. Such a problem is an extension of the one studied in [33], in the sense that also negative values of the parameter are allowed.*
First, we show how to discretize the problem in a way that is suitable to perform numerical continuation methods and obtain the associated bifurcation diagrams. Then, we analyze the results of the simulations, also studying the stability of the solutions.

Keywords: Superlinear indefinite problems, numerical global bifurcation diagrams, high multiplicity of positive solutions, stability, Neumann boundary conditions.
MS Classification 2010: 65L10, 65L60, 65P30, 65L07.

1. Introduction

The term *superlinear indefinite problems* is used in the literature to refer to nonlinear boundary value problems of elliptic type which are characterized by the presence of a sign-changing nonlinearity. These problems have attracted the attention of many researches in the last decades, since they have revealed a wide phenomenology of multiplicity of positive solutions. We refer to [1, 3–6, 16, 20, 21, 29, 31] for some pioneering works, to the book [22] for some related results (see, in particular, Chapter 9), and to the monograph [10] for an extended review on the existing literature, up to the most recent one.

In [28], we have considered, together with J. López-Gómez and F. Zanolin,

the following one-dimensional problem with Dirichlet boundary conditions

$$\begin{aligned} u'' &= \quad u + a(t)u^p; \quad t \ 2 \ (0;1), \\ u(0) &= u(1) = M; \end{aligned} \tag{1}$$

with $\quad < 0, p > 1$ (which makes the problem superlinear), and the weight $a(t)$ defined as the piecewise constant function

$$a(t) = \begin{array}{ll} c; & \text{for } t \ 2 \ (0; \quad) \ [\ (1 \quad ;1), \\ b; & \text{for } t \ 2 \ (\ ;1 \quad), \end{array} \tag{2}$$

where $\quad 2 \quad 0; \frac{1}{2}$ and $b; c > 0$. Thus, it is apparent that problem is indefinite. As for the boundary condition, M is taken in $(0; +1]$ and, when $M = +1$, the condition is understood in the limiting sense and gives rise to the so called *large* or *blow-up solutions*.

The main result of [28] is that problem (1) admits, for certain values of the parameters, an arbitrarily high number of positive solutions. We mention that a different mechanism for obtaining high multiplicity of positive solutions for superlinear indefinite problems had been previously observed numerically in [16], and analytically proved - in a different setting - in [7, 8, 12, 13, 15]. Nonetheless, these results substantially differ from the one of [28], since the multiplicity was originated by the high number of positive parts of the weight. Instead, [28] is the first work where a high multiplicity result has been obtained with weights having only one positive part (cf. (2)).

In addition, the fact of considering the piecewise constant weight (2) allowed us in [28] to determine the structure of the global bifurcation diagrams, which become more and more complex (i.e., they exhibit an increasing number of turning points and secondary bifurcations) as the number of solutions increases. Such bifurcation diagrams have been obtained analytically, and the value of the weight in the positive part, b, has been used as a main continuation parameter, an idea that originally goes back to [21].

To complete the reference to previous results related to problem (1), we mention [27], where with J. López-Gómez we considered, in place of (2), an asymmetric weight, which entailed a break-up of the bifurcation diagrams into several connected components, and [32], where we studied the relation between the symmetric and asymmetric case in a neighborhood of the bifurcation points. Finally, in [24], together with J. López-Gómez and M. Molina-Meyer, we considered the same problem in a bounded domain $\Omega \quad \mathbb{R}^N$, $N \quad 1$, and obtained general (minimal) multiplicity results in that context, also studying the stability of the solutions.

The numerical computation of the complex bifurcation diagrams arising in such situation has turned to be an intricate question, since the increasing number of singular points (secondary bifurcations and turning point) which were

closer and closer one to each other required some refinements in the algorithms. We refer to [23, 25, 26] for these numerical aspects.

In [33], instead, we have considered the superlinear indefinite problem with homogeneous Neumann boundary conditions

$$\begin{aligned} u'' &= -u + a(t)u^p; \quad \text{for } t \in (0;1), \\ u'(0) &= u'(1) = 0; \end{aligned} \tag{3}$$

This change made the use of b as a continuation parameter no longer possible. Instead, we used the parameter α, which measures the *amplitude* of the positive part of the weight; this idea was suggested by [18]. The main results of [33] can be summarized as follows (see also Figure 1, which is taken from [33]).

THEOREM 1.1 ([33], Theorem 5.1). *Let* $\beta_n := \frac{(n\pi)^2}{p-1}$, $n \in \mathbb{N}$, *and assume that* $\beta \in [\beta_{n+1}; \beta_n)$ *for some* $n \in \mathbb{N}$. *Then:*

(i) if $n = 0$, *the minimal bifurcation diagram in* $\mathcal{D}$ *for problem* (3) *consists of a curve starting from* $(\alpha = 0)$ *and bifurcating from* $+\infty$ *at* $\lambda = 1/2$. *Such a curve, that contains symmetric solutions, will be referred to as* principal curve *(see Figure 1(A));*

(ii) if $n = 1$, *the minimal bifurcation diagram in* $\mathcal{D}$ *for problem* (3) *consists of one component containing the principal curve with two additional branches, containing asymmetric solutions, that start from* $(\alpha = 0)$ *and merge in a bifurcation point on the principal curve (see Figure 1(B));*

(iii) if $n = 2k+1$, $k \in \mathbb{N}$, *the minimal bifurcation diagram in* $\mathcal{D}$ *for problem* (3) *consists of* $k+1$ *components: one, as in (ii), containing the principal curve with two branches bifurcating from it and reaching the axis* $(\alpha = 0)$, *plus* k *additional bounded components, each formed by four branches (two with symmetric solutions and two with asymmetric solutions) that start from the axis* $(\alpha = 0)$ *and three of which merge in a bifurcation point, while (at least) two of them merge in a subcritical turning point (see Figure 1(D));*

(iv) if $n = 2k$, $k \in \mathbb{N}$, *the minimal bifurcation diagram in* $\mathcal{D}$ *for problem* (3) *consists of* $k+1$ *components: one, as in (ii), containing the principal curve with two branches bifurcating from it and reaching the axis* $(\alpha = 0)$, $k \geq 1$ *bounded components as in (iii), each consisting of four branches (two with symmetric solutions and two with asymmetric solutions) that start from* $(\alpha = 0)$ *and form a subcritical turning point and a bifurcation point, and an additional bounded component formed by two branches of symmetric solutions that start from the axis* $(\alpha = 0)$ *and merge in a subcritical turning point (see Figure 1(C));*

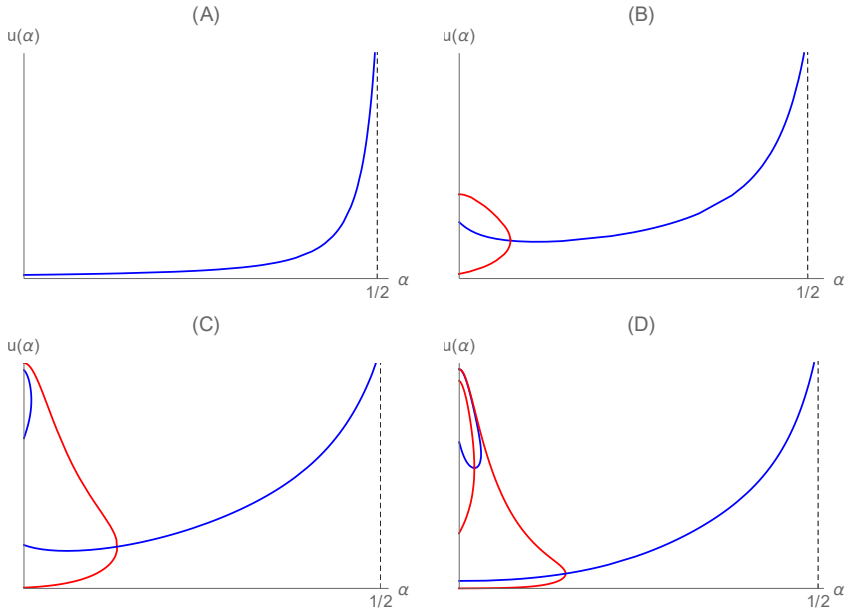

Figure 1: Bifurcation diagrams in for problem (3) corresponding to the following cases: (A) 2 [1; 0), (B) 2 [2; 1), (C) 2 [3; 2), (D) 2 [4; 3). The blue branches are formed by symmetric solutions, the red ones by asymmetric solutions.

In particular, the previous result establishes that the bifurcation diagrams in , with 0, are always non connected for sufficiently negative 's (precisely, for < 2), which was not the case in [28]. However, one may think that this non-connectedness is only apparent and is due to the fact that in [33] we only considered 0. Indeed, one can extend the problem also for negative 's, and might think that the several branches combine to form a connected diagram, like the ones of [28].

One of the main goals of this work is to give numerical evidence that this does not happen, and the global diagrams of the extended problem remain disconnected. In addition, with our numerical study, we will analyze the stability of the solutions of the problem.

In order to extend problem (3) for < 0, first of all, we extend the weight as follows

$$a_1(t) = \begin{cases} c; & \text{for } t \in (\ ;0) \cup (1;1\ \ ), \\ b; & \text{for } t \in (0;1), \end{cases} \qquad < 0:$$

Then, we impose the Neumann boundary conditions on the boundary of the new domain, arriving at

$$\begin{array}{l} u'' = \quad u + a_1(t)u^p; \qquad t \in (\ ;1\ \ \ ), \\ u'(\ \ ) = 0 = u'(1\ \ \ ); \end{array} \qquad < 0. \tag{4}$$

A motivation for considering such a boundary condition arises from the biological interpretation of superlinear indefinite problems, which can be used to describe the stationary states of the evolution of the density of a population, taking into account intra-specific competition, according to the classical logistic model, in the regions where the weight is negative, and intra-specific facilitative effects in the region where the weight is positive. Under this perspective, Neumann boundary conditions describe the fact that the habitat is isolated and no inner or outer flux of individuals takes place.

One of the main issues to numerically deal with problems (3) and (4) is the fact that the bifurcation parameter does not appear explicitly in the differential equations, but only implicitly in its domain. Indeed, for the numerical continuation methods one has to differentiate the approximating problem with respect to the bifurcation parameter. For this to be possible, one cannot use the collocation procedure, used in [23, 25, 26] to compute the bifurcation diagrams in b for problem (1), which is very efficient from the computational point of view. Instead, as suggested by [30], one can use a Galerkin method which makes the differentiation with respect to treatable, but entails the disadvantage of being much slower for the computations.

In Section 2 we present such a method to discretize problem (4) and in Section 3 we present the results of the numerical experiments that we have performed, using the obtained discretization. Finally, in Section 4, we present some remarks on two different extensions of problem (3) for < 0.

2. Discretization of problem (4)

One of the main difficulties to study problem (4) as < 0 varies is the fact that the domain grows without restrictions as becomes more and more negative. For this reason, first of all, we perform the change of variable $x = \frac{t}{1\ \ 2\ \ }$ to transform (4) into the following equivalent problem, which is set in a domain of fixed size:

$$\begin{array}{l} \frac{1}{(1\ \ 2\ \ )^2} u'' = \quad u + a_2(x)u^p; \qquad x \in (0;1), \\ u'(0) = 0 = u'(1); \end{array} \tag{5}$$

where the $'$ now indicates derivatives with respect to x and

$$a_2(x) := a_1(t(x)) = \begin{cases} c; & \text{for } x \in \ 0; \frac{}{1\ \ 2\ \ } \ [\ \ \frac{1}{1\ \ 2\ \ }; 1\ \ , \\ b; & \text{for } x \in \ \frac{}{1\ \ 2\ \ }; \frac{1}{1\ \ 2\ \ }\ \ , \end{cases} \qquad < 0.$$

We observe that problem (5) shares some features with (3): both are superlinear indefinite problems set in $(0;1)$ with homogeneous Neumann boundary conditions, and in both cases the position of the points of discontinuity of the weight varies with α. Moreover, for $\alpha = 0$, both problems reduce to the same purely superlinear one, i.e., with a positive weight. Nonetheless, their behavior with respect to α might be substantially different, since the coefficient in front of the second derivative in (5) also depends on α, while it is constant in (3). Equivalently, (5) can be seen as a variant of (3) in which α and the values of the weight depend on α. In the light of Theorem 1.1, the number of solutions of (3) depends on the value of α, thus it is not easy to relate one problem to the other.

Since the analysis is not easy, we perform numerical simulations to get insight into problem (5) and, hence, on the equivalent problem (4). To do so, we have to discretize (5). We consider $p = 2$ and, as suggested by [30], we apply a Fourier–Galerkin method. It consists in approximating a solution $u(x)$ by the truncated Fourier series

$$\overline{u}(x) = \sum_{j=1}^{n} u_j \, \varphi_j(x); \qquad \text{where} \quad \varphi_j(x) := \cos((j-1)\pi x), \tag{6}$$

in multiplying the differential equation of (5) by the i-th element of the Fourier basis $\varphi_i(x)$, and in integrating over $(0;1)$. In this way, we obtain the i-th equation of the discretized problem, which will be denoted by F_i, and the unknown is now the vector of Fourier coefficients $\mathbf{u} = (u_j)_{j=1}^{n} \in \mathbb{R}^n$, considered as a column vector. The fact of taking only cosine terms in (6) is due to the boundary conditions in (5). Hence, the equation F_i, $1 \le i \le n$, reads

$$\begin{aligned} &\sum_{j=1}^{n} \frac{(j-1)^2}{2} \, u_j \int_0^1 \varphi_j(x)\,\varphi_i(x)\,dx \\ &\quad - c \int_0^{\frac{\alpha}{1-2\alpha}} \Big(\sum_{j=1}^{n} u_j \, \varphi_j(x) \Big) \varphi_i(x)\,dx + b \int_{\frac{\alpha}{1-2\alpha}}^{\frac{1-\alpha}{1-2\alpha}} \Big(\sum_{j=1}^{n} u_j \, \varphi_j(x) \Big) \varphi_i(x)\,dx \\ &\quad - c \int_{\frac{1-\alpha}{1-2\alpha}}^{1} \Big(\sum_{j=1}^{n} u_j \, \varphi_j(x) \Big) \varphi_i(x)\,dx. \end{aligned} \tag{7}$$

On the one hand, the orthogonality conditions give

$$\int_0^1 \varphi_j(x)\,\varphi_i(x)\,dx = \begin{cases} 1 & \text{if } i = j = 1, \\ 1/2 & \text{if } i = j > 1, \\ 0 & \text{otherwise,} \end{cases}$$

on the other one we observe that

$$\left(\sum_{j=1} u_j \ _j(x)\right)^2 = \left(\sum_{j=1} u_j \ _j(x)\right)\left(\sum_{k=1} u_k \ _k(x)\right) = \sum_{j=1}\sum_{k=1} u_j u_k \ _j(x) \ _k(x);$$

and that

$$\begin{aligned} 4 \ _i(x) \ _j(x) \ _k(x) = &\cos((i+j+k \quad 3) \ x) + \cos((i+j \quad k \quad 1) \ x) \\ &+ \cos((i \quad j+k \quad 1) \ x) + \cos((i \quad j \quad k+1) \ x); \end{aligned}$$

thus, if we set

$$h^{i;1}_{jk}(x) = \begin{cases} x & \text{if } i+j+k=3, \\ \frac{\sin((i+j+k \quad 3) \ x)}{(i+j+k \quad 3)} & \text{otherwhise,} \end{cases}$$

$$h^{i;2}_{jk}(x) = \begin{cases} x & \text{if } i+j \quad k=1, \\ \frac{\sin((i+j \quad k \quad 1) \ x)}{(i+j \quad k \quad 1)} & \text{otherwhise,} \end{cases}$$

$$h^{i;3}_{jk}(x) = \begin{cases} x & \text{if } i \quad j+k=1, \\ \frac{\sin((i \quad j+k \quad 1) \ x)}{(i \quad j+k \quad 1)} & \text{otherwhise,} \end{cases}$$

$$h^{i;4}_{jk}(x) = \begin{cases} x & \text{if } i \quad j \quad k= \quad 1, \\ \frac{\sin((i \quad j \quad k+1) \ x)}{(i \quad j \quad k+1)} & \text{otherwhise,} \end{cases}$$

we have that a primitive of $ _i(x) \ _j(x) \ _k(x)$ is

$$h^i_{jk}(x) := \frac{1}{4}\left(h^{i;1}_{jk}(x) + h^{i;2}_{jk}(x) + h^{i;3}_{jk}(x) + h^{i;4}_{jk}(x)\right) :$$

As a consequence, (7) reads

$$\begin{aligned} &\sum_{j=1} \frac{(j \quad 1)}{1 \quad 2}{}^2 \left(\int_0^1 u_j \ _j(x) \ _i(x) \, dx\right. \\ &\quad c\left(\sum_{j=1}\sum_{k=1} u_j \ h^i_{jk} \ \frac{}{1 \quad 2} \ h^i_{jk}(0) \ u_k\right) \\ &\quad + b\left(\sum_{j=1}\sum_{k=1} u_j \ h^i_{jk} \ \frac{1}{1 \quad 2} \ h^i_{jk} \ \frac{}{1 \quad 2} \ u_k\right) \\ &\quad c\left(\sum_{j=1}\sum_{k=1} u_j \ h^i_{jk}(1) \ h^i_{jk} \ \frac{1}{1 \quad 2} \ u_k\right) \end{aligned}$$

and, observing that $h^i_{jk}(0) = 0$, it reduces to

$$\sum_{j=1} \frac{(j-1)}{1/2}^2 u_j \int_0^1 \varphi_j(x)\,\varphi_i(x)\,dx + (b+c)\left(\sum_{j=1}\sum_{k=1} u_j\, h^i_{jk}\,\frac{1}{1/2}\, h^i_{jk}\,\frac{}{1/2}\, u_k\right) - c\sum_{j=1}\sum_{k=1} u_j h^i_{jk}(1) u_k;$$

which leads to

$$F_1 = u_1 + (b+c)\,\mathbf{u}^t\, H^1\,\frac{1}{1/2}\, H^1\,\frac{}{1/2}\,\mathbf{u} - c\,\mathbf{u}^t H^1(1)\,\mathbf{u};$$

and, for $i > 1$,

$$F_i = \frac{(i-1)}{1/2}^2 \frac{u_i}{2} + (b+c)\,\mathbf{u}^t\, H^i\,\frac{1}{1/2}\, H^i\,\frac{}{1/2}\,\mathbf{u} - c\,\mathbf{u}^t H^i(1)\,\mathbf{u};$$

where we have set $H^i(x) := (h^i_{jk}(x))^n_{j,k=1}$ and $\mathbf{u}^t$ denotes the transposed of vector $\mathbf{u}$. As a consequence, the discretized problem is

$$F(\mathbf{u};\ ) = 0; \qquad F = (F_i)^n_{i=1}.$$

Before concluding this section, we remark that, for the numerical bifurcation algorithms that we use in our simulations, it is necessary to differentiate the discretized equations also with respect to the parameter . The advantage of employing the Fourier–Galerkin method described above consists in the fact that such a derivative can be easily computed from (7) by means of the fundamental theorem of Calculus.

3. Results of the numerical experiments

In this section we show the results of the experiments performed by applying numerical continuation methods to the discretized problem obtained in Section 2. We send the interested reader to [2, 9, 17, 19] for general references on numerical continuation methods, and to [25, 26] for more recent references where some improvements to the algorithms are performed in order to be able to compute complex bifurcation diagrams as those appearing in this work.

Structure of the bifurcation diagrams. For our numerical experiments, we have used the following values of the parameters:

$$b = c = 1; \qquad p = 2;$$

and $2 f 4; 25; 60; 120g$, which are the same values used to obtain the diagrams in Figure 1. The choice of the number of discretization points has been $n = 300$ with the aim of achieving a good precision (measured by the size of the Fourier coefficients u_j, $n \quad 10 \quad j \quad n$, whose modulus in all our simulation is smaller than 10^{-4} and, in many cases, smaller than 10^{-8}) in a reasonable computational time. The resulting bifurcation diagrams are represented in Figure 2.

In particular we observe that for $= 0$ problems (3) and (4) coincide, thus the number of solutions is necessarily the same, and the branches are continuous. Moreover, the global patterns of the branches for < 0 are the same as those for > 0 described in Theorem 1.1, the only difference being that the principal curve seems to be continuable for all < 0.

To understand this difference, we observe that a necessary condition for (3) and (4) to possess positive solutions, which can be easily obtained by integrating the differential equation and using the boundary conditions, is that the weight has to change sign. This condition is no longer true for problem (3) when $= \frac{1}{2}$, thus all the solutions are lost before such a value of the parameter is reached. Instead, the weight in (4) changes sign for all < 0, thus no restrictions exist on , and actually our simulations suggest that existence occurs for all < 0.

Moreover, we observe that the diagrams are non-connected for sufficiently negative 's and the number of connected components increases as becomes more and more negative.

This is not a priori evident, since, as commented above, problem (5) can be equivalently written as

$$u'' = \tilde{}( )u + (1 \quad 2)^2 a_2(x)u^p; \qquad x 2 (0;1),$$

with $\tilde{}( ) = (1 \quad 2)^2$, and we have the following opposite trends coinciding as $! \quad 1$:

i) first, as above, the positive part of the weight, whose size is $\frac{1}{1 \quad 2}$, becomes smaller and smaller, thus the necessary condition for the existence of solutions - the change of sign of the weight - tends to be violated, though it is so only in the limiting case $= \quad 1$. This makes one infer that the solutions are lost as < 0 decreases;

ii) contrastingly, the value of $\tilde{}( )$ goes to 1 as $! \quad 1$, thus, if all the other parameters were fixed, Theorem (1.1) would guarantee the existence of an increasing number of solutions. Nonetheless, the values of for

which such a high number of solution is present depends on : essentially, one should study the dependence of the turning points on , which is a very interesting open problem both from the analytical and the numerical point of view;

iii) finally, the values of the weight, both in the negative and the positive part, go to $+\infty$ as $\to 1$, and the overall effect is not clear in this case (cf. [11] for a similar problem).

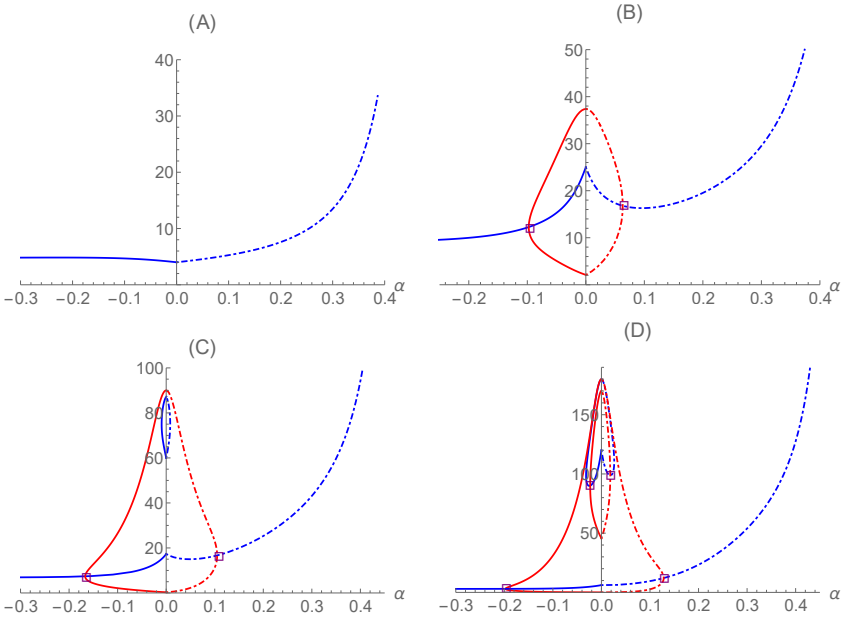

Figure 2: Numerical bifurcation diagrams in obtained for problem (3) (> 0, with dash-dotted line) and problem (4) (< 0, with continuous line) corresponding to the following values of :

(A) $= 4$, (B) $= 25$, (C) $= 60$, (D) $= 120$.

On the vertical axes we plot the values of $u(\ )$ for > 0 and $u(0)$ for < 0, i.e. we represent the value of the solution where the weight changes sign for the first time. As in Figure 1, the blue branches are formed by symmetric solutions, while the red ones by asymmetric solutions. The bifurcation points have been marked with squares.

REMARK 3.1: A natural question, that arises after the comments performed above on the general properties of the bifurcation diagram, is whether the branches are differentiable, with respect to , at = 0. By using a finite difference method, the results that we obtain for the approximation of the left and right derivatives of the several branches appearing in the diagrams of Figure 2 have been gathered in Table 1.

	Point	Right derivative	Left derivative
-4	(0; 4:00000)	10.2952	-10.2952
-25	(0; 2:09423)	63.8469	-42.0332
-25	(0; 25:0000)	-333.815	333.815
-25	(0; 37:3889)	-4.71944	2.46041
-60	(0; 0:311947)	14.5182	-9.67665
-60	(0; 17:3092)	-129.934	290.669
-60	(0; 60:0000)	1040.64	-1040.64
-60	(0; 87:1313)	-312.416	262.173
-60	(0; 89:9989)	10.861	-10.8944
-120	(0; 0:0251730)	1.72774	-1.17619
-120	(0; 6:14466)	-7.37161	76.2526
-120	(0; 45:5856)	1197.07	-765.859
-120	(0; 120:000)	-2503.6	2503.6
-120	(0; 170:378)	-432.671	262.252
-120	(0; 179:797)	16.8713	-21.3551
-120	(0; 180:000)	43.8456	-43.8475

Table 1: Values of the derivatives with respect to of the branches in the bifurcation diagrams of Figure 2, evaluated at = 0.

As we can see from the previous table, the right derivative always has the opposite sign of the left one; thus, our numerical simulations suggest that none of the branches is differentiable at = 0. Moreover, we see that, at the points (0;), with $2 f 4; 25; 60; 120g$, the right and the left derivative have the same absolute value. In view of this, we conjecture that, for all < 0, the following relation holds true:

$$\frac{d}{d}\hat{u}\ (0; \ )\ _{=0^+} = \frac{d}{d}\hat{u}\ (0; \ )\ _{=0} ; \tag{8}$$

where $\hat{u}\ (; \ )$ is the unique solution of (3) for > 0 and (4) for < 0 such that $u\ (0; 0) =$. To try to prove this relation, one could perform some asymptotic expansions for 0, in the spirit of the ones - carried out in a completely different context - of [11, Section 7], but this goes outside the scope of this work, and we leave it as an open question.

Stability of the solutions. As established in [14, Theorem 3.8], problems (3) and (4) do not admit any positive stable solutions, since $\lambda < 0 = \lambda_0$ (we use the same notation of [14] and denote by λ_0 the principal eigenvalue of the linearized problem at $u = 0$).

Here, we study the linear stability of the solutions of (5) following [9], i.e. by considering the parabolic counterpart of (5)

$$u_t - \frac{1}{(1-\varepsilon^2)^2} u_{xx} = \lambda u + a_2(x) u^p, \qquad t > 0, \quad x \in (0,1) \tag{9}$$

taking time-dependent approximating functions

$$\overline{u}(t,x) = \sum_{j=1}^{N} u_j(t)\, \varphi_j(x),$$

and obtaining, by reasoning as in Section 2, a system of ordinary differential equations for the unknown functions $u_j(t)$. This nonlinear system is then linearized around a steady state of (9), i.e. a solution of (5), and the dimension of the unstable manifold of such a steady state corresponds to the number of eigenvalues of the linearization having positive real part.

The observed stability patterns can be summarized as follows and are illustrated in Figure 3 (we use the notation of Theorem 1.1 and assume that $\varepsilon \in [\varepsilon_{n+1}, \varepsilon_n)$ for some $n \in \mathbb{N}$):

- for $\varepsilon = 0$, problem (5) has $2n+1$ solutions. We denoted them by $u^{(i)}$, $i = 1, 2, \dots, 2n+1$, (we use superscripts in order not to confuse them with the coefficients of the Fourier expansions used above) so that

  $$u^{(1)}(0) < u^{(2)}(0) < \dots < u^{(2n+1)}(0).$$

  For all $i = 1, 2, \dots, n+1$, the dimension of the unstable manifold of the solution $u^{(i)}$ coincides with the one of the solution $u^{(2n+2-i)}$ and equals i;

- on the branches of asymmetric solutions (represented in red in Figure 3), the dimension of the unstable manifold of the solution does not change;

- on the branches of symmetric solutions (represented in blue in Figure 3), the dimension of the unstable manifold changes by 1 as a bifurcation or a turning point is crossed, monotonically on each branch. Moreover, the unique solution of the problem for $\lambda > 1$, which lies on the principal branch, has a 1-dimensional unstable manifold.

We point out that the observed stability patterns for problem (3) with $\varepsilon > 0$ are exactly the same.

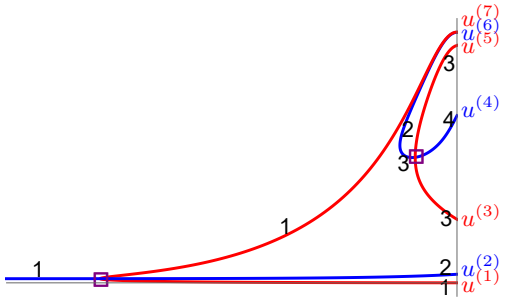

Figure 3: Dimensions of the unstable manifold for the solutions of problem (4) with $= 120$ 2 [$_4$; $_3$) (case (D) of Figure 2).

Profiles of the solutions. To conclude the presentation of the results of our numerical experiments, we plot in Figure 4 the profiles of the solutions in a case of high multiplicity, corresponding to the values of the parameters that give rise to the bifurcation diagram of Figure 2(D).

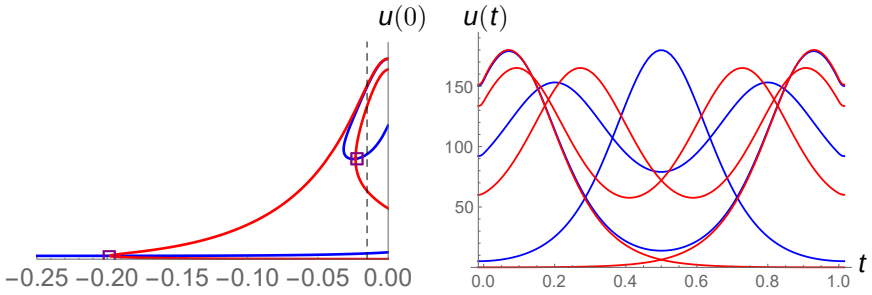

Figure 4: Bifurcation diagram in for problem (4) with $= 120$ (left) and profiles of the seven solutions of the problem for $= 0{:}015$ (right). The level $= 0{:}015$ has been marked in the bifurcation diagram with a dashed line. Observe that the position of each solution of the right plot can be determined in the bifurcation diagram, at the level $= 0{:}015$, from its value at $t = 0$ and its symmetry.

Moreover, in order to make apparent that the behavior of the solutions is similar for positive and negative 's, we now present a description of the behavior of the solutions along each of the branches of the bifurcation diagram. Once again, we present the plots corresponding to the bifurcation diagram of Figure 2(D), since it is the most illustrative one.

Figure 5 shows the plots of some solutions on the upper blue branch in

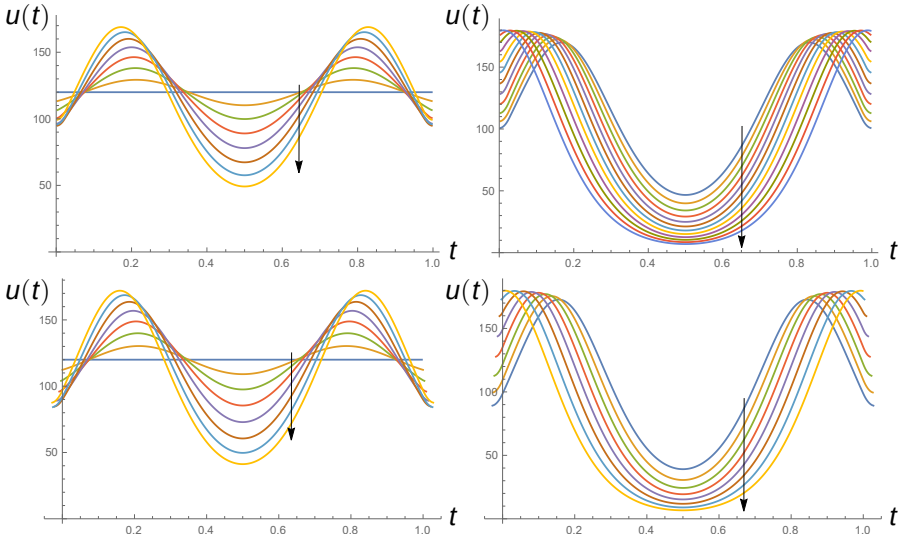

Figure 5: Plots of some solutions on the upper blue branch in Figure 2(D): upper row for $\quad > 0$, lower row for $\quad < 0$. The arrows indicate the direction in which the bifurcation diagram has been gone through, according to the description in the text.

Figure 2(D), that connects the point $(0; 120)$ to the point $(0; 179{:}797)$ in the bifurcation diagram. All the solution on this branch are symmetric. In the upper row of Figure 5 we represent the solutions for $\quad > 0$: in the left plot we start from the constant solution corresponding to the point $(0; 120)$ in the bifurcation diagram and arrive to the turning point, which occurs at $(0{:}0263530; 110{:}425)$, while in the right plot the solutions go from the turning point to the upper point $(0; 179{:}797)$. In the lower row of the figure, instead, we represent the solutions for $\quad < 0$ according to the same pattern: in the left plot from the point $(0; 120)$ to the turning point $(\quad 0{:}0316540; 98{:}6296)$, and in the right plot from the turning point to the upper point $(0; 179{:}797)$. The arrows in the figure visually indicate the direction along which the solutions evolve on the bifurcation diagram, following the starting and the endpoint specified in the previous description.

Figure 6 shows the plots of some solutions on the lower blue branch in Figure 2(D), starting from $(0; 6{:}14466)$: the upper plot is for $\quad > 0$ and the lower ones for $\quad < 0$. All the solutions are, again, symmetric. In the lower left plot we represent the solutions after the change of variables that transforms the domain $(\quad ; 1 \quad)$, which varies with $\quad$, in the fixed domain $(0; 1)$, while in the right plot we use the original domain of problem (4). This has been done

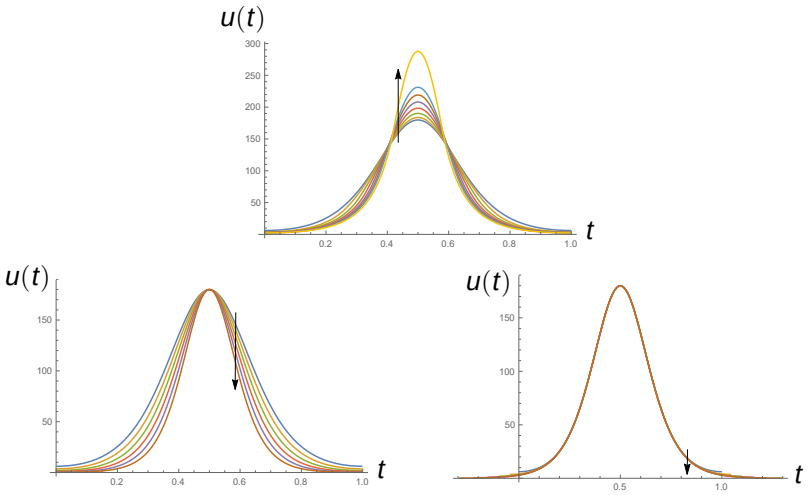

Figure 6: Plots of some solutions on the lower blue branch in Figure 2(D), starting from (0; 6:14466). The upper plot is for > 0, the lower left plot for < 0, working with fixed domain $(0; 1)$, and the lower right plot for > 0 with the original domain of problem (4).

because the difference between the different solutions is amplified in the fixed domain.

In Figure 7 we represent the solutions that lie on the red branch of Figure 2(D) starting from (0; 0:0251730) and arriving at (0; 180:000): on the upper row the ones for > 0 and on the lower row the ones for < 0. All the solutions, apart from the ones on the bifurcation points (0:197821; 3:03203) and (0:128325; 12:0364), are asymmetric. The left plots go from the starting point (0; 0:0251730) on the bifurcation diagram up to the bifurcation point, while the ones on the right go from the bifurcation point to the ending point (0; 180:000).

Finally, in Figure 8 we represent the solutions that lie on the other red branch of Figure 2(D), starting from (0; 45:5856), arriving at (0; 170:378) and following the same patterns used in Figure 7: top left for > 0 up to the bifurcation point (0:0194360; 98:8542), top right > 0 starting from the bifurcation point, bottom left for < 0 up to the bifurcation point (0:0234266; 90:0263) and bottom right for < 0 starting from the bifurcation point.

4. Final remarks

To conclude this work, we observe that we may extend problem (3) also in other different ways than the one considered above. A first possibility consists in maintaining the condition on the derivatives at the fixed points $t = 0$ and

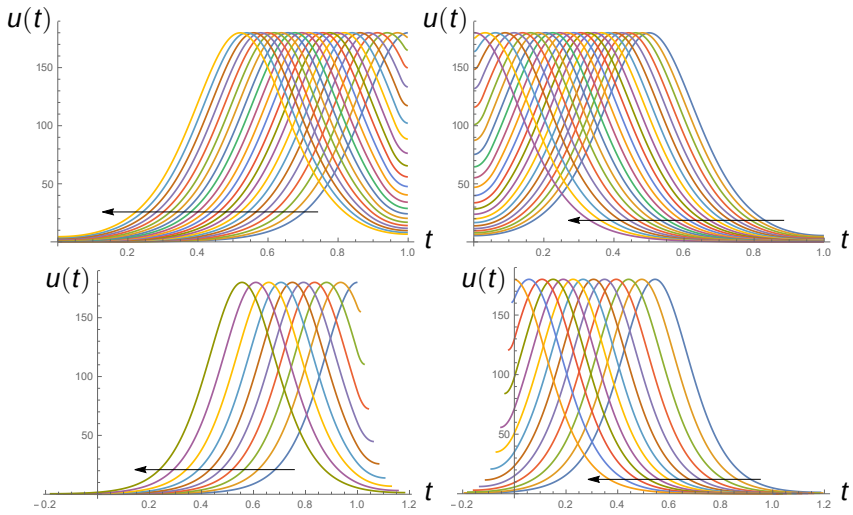

Figure 7: Plots of some solutions on the red branch in Figure 2(D) starting from $(0; 0.0251730)$. The upper plots are for $\quad > 0$, the lower ones for $\quad < 0$. The left plots represent, in the direction of the arrows, the solutions from the starting point to the bifurcation points, where they become symmetric, while in the right ones we start from the bifurcation points and arrive at $(0; 180.000)$.

$t = 1$, obtaining

$$\begin{array}{l} u'' = \quad u + a_1(t)u^p; \qquad t \in (\quad ; 1 \qquad), \\ u'(0) = 0 = u'(1); \end{array} \qquad < 0. \tag{10}$$

Doing so, we no longer have to deal with a boundary value problem, but with an "intermediate" value problem.

This problem is less interesting, since one readily observes that its solutions are in 1-1 correspondence with the solutions of the purely superlinear Neumann problem

$$\begin{array}{l} u'' = \quad u + bu^p; \qquad t \in (0; 1); \\ u'(0) = 0 = u'(1). \end{array} \tag{11}$$

Indeed, one takes any solution $\overline{u}$ of (11) and extends it to $(\quad ; 0)$ and $(1; 1 \qquad)$ with the unique solutions of the initial value problems

$$\begin{cases} u'' = \quad u \quad cu^p; \quad t \in (\quad ; 0); \\ u(0) = \overline{u}(0); \\ u'(0) = 0; \end{cases} \qquad \begin{cases} u'' = \quad u \quad cu^p; \quad t \in (1; 1 \qquad); \\ u(1) = \overline{u}(1); \\ u'(1) = 0; \end{cases} \tag{12}$$

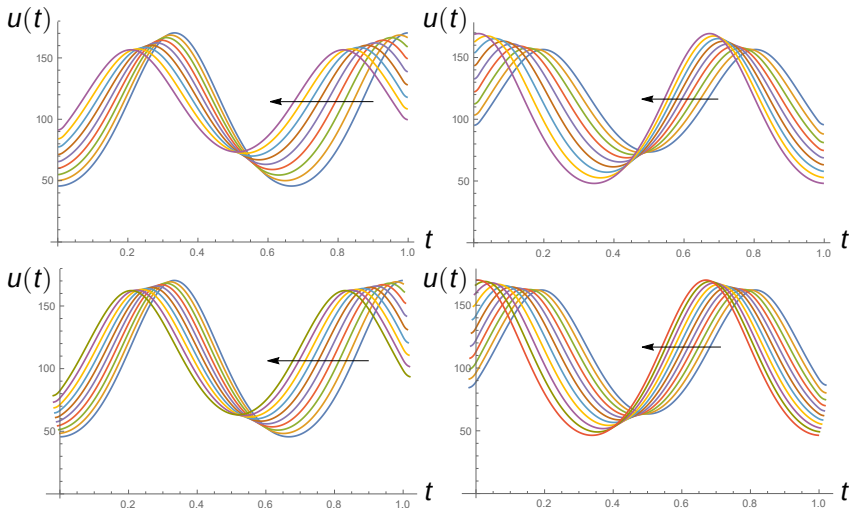

Figure 8: Plots of some solutions on the red branch in Figure 2(D) starting from $(0; 45.5856)$. The upper plots are for $\quad > 0$, the lower ones for $\quad < 0$. The left plots represent, in the direction of the arrows, the solutions from the starting point to the bifurcation points, where they become symmetric, while in the right ones we start from the bifurcation points and arrive at $(0; 170.378)$.

respectively. In this way, a solution of (10) is obtained. For this reason, we can say that the extension (10) makes the problem lose its indefinite nature. Nonetheless, we remark that the existence of global solutions for problems (12) depends on the values of $\quad$, since the solutions blow up in finite time, which has to be compared with $\quad$. By studying such a blow-up time, one can also construct the bifurcation diagrams in $\quad$ of problem (10). This can be done with the elements developed in [33].

A second possible extension is the following one

$$\begin{array}{l} u'' = \quad u + a_3(t)u^p; \qquad t \in (2 \quad ; 1 \quad 2 \quad), \\ u'(2 \quad) = 0 = u'(1 \quad 2 \quad); \end{array} \qquad < 0; \tag{13}$$

with

$$a_3(t) := \begin{array}{ll} c; & \text{for } t \in (2 \quad ; \quad) \cup (1 \qquad ; 1 \quad 2 \quad), \\ b; & \text{for } t \in (\quad ; 1 \qquad). \end{array}$$

This problem cannot be directly related to the one extensively studied above, since, here, both the size of the positive part of the weight and of the negative one vary with $\quad$.

To study this problem numerically, we first had to slightly modify the discretization performed in Section 3. Once that done, we have computed the

corresponding bifurcation diagrams and the related profiles of the solutions. The results of our computations have been represented in Figures 9 and 10.

The left plot of Figure 9 shows the bifurcation diagram of problem (13) with = 120. By comparing it with the right part of the diagram in Figure 2(D), which corresponds to the same value of , we observe that the qualitative structure of the bifurcation diagrams is similar for the two extensions.

Nevertheless, a closer look at it (see the right plot of Figure 9) shows that some differences arise in the quantitative behavior of the bifurcation diagram. Indeed, some of the branches are not monotone, which does not occur for the corresponding ones in Figure 2(D). Moreover, in the left plot of Figure 9 we have marked only one bifurcation point, while in Figure 2(D) there were two of them. We think that this is uniquely due to the fact that we have not been able to perform the simulations for sufficiently negative values of , since the solutions on the three branches are very close to each other apart from being very small. We conjecture, that the qualitative shape of the diagram for problem (13) is exactly as for problem (4) and that, if one is able to continue the simulations for more negative 's, the bifurcation point should arise. In order to do so, one may try to apply the treatment of narrow turning points developed in [26].

Finally, if we compare the plots of the solutions of problem (13), which are shown in Figure 10, with the corresponding ones of problem (4) (see Figures 5–8), we observe that they also follow the same qualitative patterns.

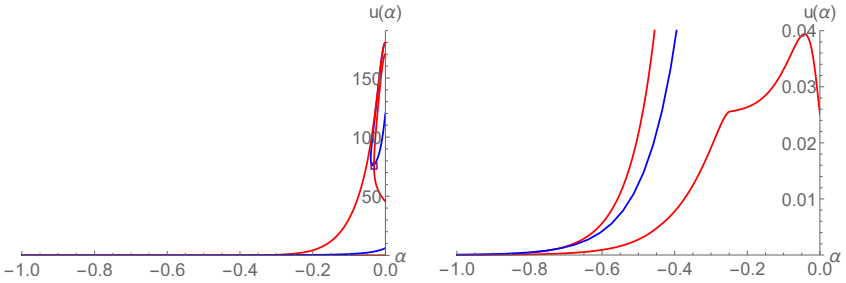

Figure 9: Bifurcation diagram of problem (13) for = 120 (left) and a zoom of its lower part (right).

Acknowledgment

The author is supported by the Spanish Ministry of Science, Innovation and Universities through project PGC2018-097104-B-100. He also wishes to thank the anonymous referee for his/her valuable comments, that led to a substantial

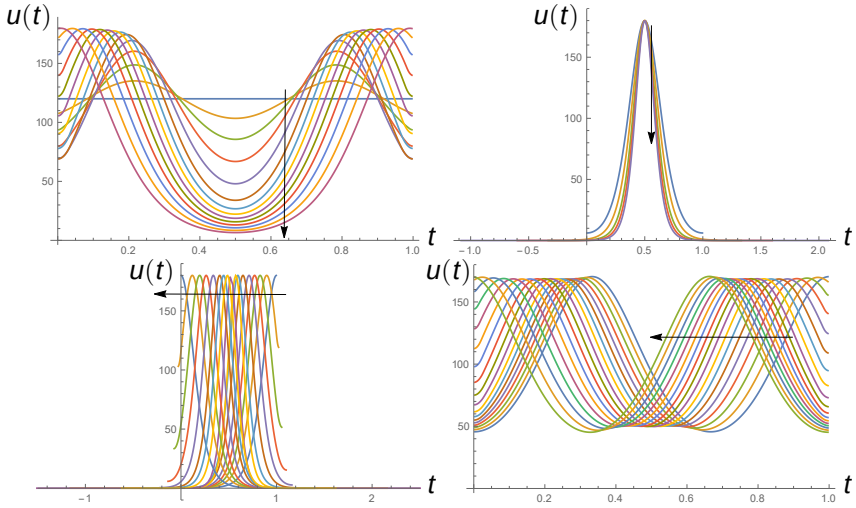

Figure 10: Plots of some solutions related to the left diagram of Figure 9: on the upper blue branch (top left), on the lower blue branch (top right), on the biggest red branch (bottom left) and on the smallest red branch (bottom right). The arrows indicate how the solutions evolve as the bifurcation diagrams are gone though, as described in the text of Section 3 and as marked in the corresponding plots of the solutions of problem (4).

improvement of this work: in particular, the suggestions related to the figures and to consider the extended problem (13).

References

[1] S. Alama and G. Tarantello, *Elliptic problems with nonlinearities inde nite in sign*, J. Funct. Anal. **141** (1996), no. 1, 159{215.

[2] E. L. Allgower and K. Georg, *Introduction to numerical continuation methods*, Classics in Applied Mathematics, vol. 45, Society for Industrial and Applied Mathematics (SIAM), Philadelphia, PA, 2003, Reprint of the 1990 edition [Springer, Berlin].

[3] H. Amann and J. López-Gómez, *A priori bounds and multiple solutions for superlinear inde nite elliptic problems*, J. Di erential Equations **146** (1998), no. 2, 336{374.

[4] C. Bandle, M. A. Pozio, and A. Tesei, *Existence and uniqueness of solutions of nonlinear Neumann problems*, Math. Z. **199** (1988), no. 2, 257{278.

[5] H. Berestycki, I. Capuzzo-Dolcetta, and L. Nirenberg, *Superlinear inde nite elliptic problems and nonlinear Liouville theorems*, Topol. Methods Non-

linear Anal. **4** (1994), no. 1, 59{78.
[6] H. Berestycki, I. Capuzzo-Dolcetta, and L. Nirenberg, *Variational methods for inde nite superlinear homogeneous elliptic problems*, NoDEA Nonlinear Di erential Equations Appl. **2** (1995), no. 4, 553{572.
[7] D. Bonheure, J. M. Gomes, and P. Habets, *Multiple positive solutions of superlinear elliptic problems with sign-changing weight*, J. Di erential Equations **214** (2005), no. 1, 36{64.
[8] A. Boscaggin, *A note on a superlinear inde nite Neumann problem with multiple positive solutions*, J. Math. Anal. Appl. **377** (2011), no. 1, 259{268.
[9] J. C. Eilbeck, *The pseudospectral method and path following in reaction-di usion bifurcation studies*, SIAM J. Sci. Statist. Comput. **7** (1986), no. 2, 599{610.
[10] G. Feltrin, *Positive solutions to inde nite problems. A topological approach*, Frontiers in Mathematics, Birkhauser/Springer, Cham, 2018.
[11] G. Feltrin, E. Sovrano, and A. Tellini, *On the number of positive solutions to an inde nite parameter-dependent Neumann problem*, In preparation.
[12] G. Feltrin and F. Zanolin, *Existence of positive solutions in the superlinear case via coincidence degree: the Neumann and the periodic boundary value problems*, Adv. Di erential Equations **20** (2015), no. 9-10, 937{982.
[13] G. Feltrin and F. Zanolin, *Multiple positive solutions for a superlinear problem: a topological approach*, J. Di erential Equations **259** (2015), no. 3, 925{963.
[14] S. Fernández-Rincón and J. López-Gómez, *The Picone identity: A device to get optimal uniqueness results and global dynamics in Population Dynamics*, Preprint available at *http://arxiv.org/abs/1911.05066*.
[15] M. Gaudenzi, P. Habets, and F. Zanolin, *A seven-positive-solutions theorem for a superlinear problem*, Adv. Nonlinear Stud. **4** (2004), no. 2, 149{164.
[16] R. Gómez-Reñasco and J. López-Gómez, *The e ect of varying coe cients on the dynamics of a class of superlinear inde nite reaction-di usion equations*, J. Di erential Equations **167** (2000), no. 1, 36{72.
[17] H. B. Keller, *Lectures on numerical methods in bifurcation problems*, Tata Institute of Fundamental Research Lectures on Mathematics and Physics, vol. 79, Published for the Tata Institute of Fundamental Research, Bombay; by Springer, Berlin, 1987, With notes by A. K. Nandakumaran and Mythily Ramaswamy.
[18] J. López-Gómez, *Personal communication*.
[19] J. López-Gómez, *Estabilidad y bifurcacion estatica. aplicaciones y metodos numericos*, Cuadernos de Matematica y Mecanica. Serie Cursos y Seminarios, vol. 4, Santa Fe, 1988.
[20] J. López-Gómez, *On the existence of positive solutions for some inde nite superlinear elliptic problems*, Comm. Partial Di erential Equations **22** (1997), no. 11-12, 1787{1804.
[21] J. López-Gómez, *Varying bifurcation diagrams of positive solutions for a class of inde nite superlinear boundary value problems*, Trans. Amer. Math. Soc. **352** (2000), no. 4, 1825{1858.
[22] J. López-Gómez, *Metasolutions of parabolic equations in population dynamics*, CRC Press, Boca Raton, FL, 2016.
[23] J. López-Gómez, M. Molina-Meyer, and A. Tellini, *Intricate bifurcation*

diagrams for a class of one-dimensional superlinear inde nite problems of interest in population dynamics, Discrete Contin. Dyn. Syst. (2013), no. Dynamical systems, di erential equations and applications. 9th AIMS Conference. Suppl., 515{524.

[24] J. López-Gómez, M. Molina-Meyer, and A. Tellini, *The uniqueness of the linearly stable positive solution for a class of superlinear inde nite problems with nonhomogeneous boundary conditions*, J. Di erential Equations **255** (2013), no. 3, 503{523.

[25] J. López-Gómez, M. Molina-Meyer, and A. Tellini, *Intricate dynamics caused by facilitation in competitive environments within polluted habitat patches*, European J. Appl. Math. **25** (2014), no. 2, 213{229.

[26] J. López-Gómez, M. Molina-Meyer, and A. Tellini, *Spiraling bifurcation diagrams in superlinear inde nite problems*, Discrete Contin. Dyn. Syst. **35** (2015), no. 4, 1561{1588.

[27] J. López-Gómez and A. Tellini, *Generating an arbitrarily large number of isolas in a superlinear inde nite problem*, Nonlinear Anal. **108** (2014), 223{248.

[28] J. López-Gómez, A. Tellini, and F. Zanolin, *High multiplicity and complexity of the bifurcation diagrams of large solutions for a class of superlinear inde nite problems*, Commun. Pure Appl. Anal. **13** (2014), no. 1, 1{73.

[29] J. Mawhin, D. Papini, and F. Zanolin, *Boundary blow-up for di erential equations with inde nite weight*, J. Di erential Equations **188** (2003), no. 1, 33{51.

[30] M. Molina-Meyer, *Personal communication*.

[31] P. H. Rabinowitz, *Pairs of positive solutions of nonlinear elliptic partial differential equations*, Indiana Univ. Math. J. **23** (1973/74), 173{186.

[32] A. Tellini, *Imperfect bifurcations via topological methods in superlinear indefinite problems*, Discrete Contin. Dyn. Syst. (2015), no. Dynamical systems, differential equations and applications. 10th AIMS Conference. Suppl., 1050{1059.

[33] A. Tellini, *High multiplicity of positive solutions for superlinear inde nite problems with homogeneous Neumann boundary conditions*, J. Math. Anal. Appl. **467** (2018), no. 1, 673{698.

Author's address:

Andrea Tellini
Universidad Politécnica de Madrid
Departamento de Matemática Aplicada a la Ingeniería Industrial, ETSIDI
Ronda de Valencia 3, 28012 Madrid, Spain
E-mail: andrea.tellini@upm.es

Received February 29, 2020
Revised August 24, 2020
Accepted September 6, 2020